Research Manuscript

Alpha-1-antitrypsin and its variant-dependent role in COVID-19 pathogenesis

Christian S Stevens[1#], Kasopefoluwa Y Oguntuyo[1#], Shreyas Kowdle[1], Luca Brambilla[1], Griffin Haas[1], Aditya Gowlikar[1], Mohammed NA Siddiquey[2], Robert M Schilke[2], Matthew D Woolard[2], Hongbo Zhang[2], Joshua A Acklin[1], Satoshi Ikegame[1], Chuan-Tien Huang[1], Jean K Lim[1], Robert W Cross[3], Thomas W Geisbert[3], Stanimir S Ivanov[2], Jeremy P Kamil[2], the Alpha-1 Foundation[4], and Benhur Lee[1]

Affiliations:

1. Department of Microbiology, Icahn School of Medicine at Mount Sinai, New York, NY 10029
2. Department of Microbiology and Immunology, Louisiana State University Health Shreveport, Shreveport, LA 71103
3. Department of Microbiology and Immunology, University of Texas Medical Branch at Galveston, Galveston, TX 77555
4. The Alpha-1 Foundation, University of Florida, Coral Gables, FL 33134

[#]These authors contributed equally to this work.

Author contributions:

CSS, KYO, and BL conceived and designed the study. CSS, KYO, SK, LB, GH, AG, MNAS, RMS, MDW, HZ, and JAA collected data. SI, CTH, JKL, JKL, RWC, TWG, SSI, and JPK contributed valuable reagents, data, and/or tools. CSS and KYO analyzed the

data and wrote the original drafts of the paper. BL reviewed the draft, supported data analysis, and provided invaluable direction throughout the conceptualization and execution of the project. All authors had the opportunity to review the manuscript prior to submission and JAA, SI, JKL, RWC, TWG, SSI, JPK provided valuable feedback during the editing process.

ABSTRACT

Rationale: SARS-CoV-2 entry into host cells is facilitated by endogenous and exogenous proteases that proteolytically activate the spike glycoprotein and antiproteases inhibiting this process. Understanding the key actors in viral entry is crucial for advancing knowledge of virus tropism, pathogenesis, and potential therapeutic targets.

Objectives: We aimed to investigate the role of naïve serum and alpha-1-antitrypsin (AAT) in inhibiting protease-mediated SARS-CoV-2 entry and explore the implications of AAT deficiency on susceptibility to different SARS-CoV-2 variants.

Findings: Our study demonstrates that naïve serum exhibits significant inhibition of SARS-CoV-2 entry, with AAT identified as the major serum protease inhibitor potently restricting entry. Using pseudoparticles, replication-competent pseudoviruses, and authentic SARS-CoV-2, we show that AAT inhibition occurs at low concentrations compared with those in serum and bronchoalveolar tissues, suggesting physiological relevance. Furthermore, sera from subjects with an AAT-deficient genotype show reduced ability to inhibit entry of both Wuhan-Hu-1 (WT) and B.1.617.2 (Delta) but exhibit no difference in inhibiting B.1.1.529 (Omicron) entry.

Conclusions: AAT may have a variant-dependent therapeutic potential against SARS-CoV-2. Our findings highlight the importance of further investigating the complex

interplay between proteases, antiproteases, and spike glycoprotein activation in SARS-CoV-2 and other respiratory viruses to identify potential therapeutic targets and improve understanding of disease pathogenesis.

KEYWORDS: COVID-19, SARS-CoV-2, alpha-1-antitrypsin, SERPINA1, alpha-2-macroglobulin, TMPRSS2, proteolytic activation, variants of concern, Omicron, Delta

60 **INTRODUCTION**

61 Severe acute respiratory syndrome coronavirus 2 (SARS-CoV-2), the causative agent
62 of coronavirus disease 2019 (COVID-19), depends on the complex interplay between
63 the virus and host for cellular entry (1–3). Understanding the various steps and factors
64 involved in viral entry is vital to our ability to successfully model the process, identify
65 potential therapeutics, and even predict genetic risk factors. For SARS-CoV-2, this
66 process is mediated by the spike glycoprotein (S). Entry involves not only the simple
67 binding interaction between spike and the entry receptor ACE2, but also the delicate
68 balance of proteases and antiproteases that contribute to proteolytic activation and
69 facilitate viral fusion (4–8). SARS-CoV-2 S undergoes two sequential proteolytic
70 activation steps: first it is cleaved at the S1/S2 polybasic site, and second it is then
71 cleaved at S2′ revealing the fusion peptide (9).
72
73 A variety of proteases are implicated in the proteolytic activation of SARS-CoV-2
74 including furin-like proteases, cathepsins, trypsin, neutrophil elastase, and TMPRSS2
75 (1, 9–16). This intricate process enables the virus to enter and fuse either at the plasma
76 membrane or within endosomes, engaging different proteases and pathways at each
77 stage. The complexities of viral entry for SARS-CoV-2 are particularly important to
78 understand, as they can be context-dependent, influenced by factors such as local
79 tissue-specific protease and antiprotease milieu, host genotype that impact these
80 milieux, and virus variants that alter susceptibility to cognate protease activation. As an
81 example of the way these relationships can develop and change over time, increasingly
82 efficient proteolytic processing and cell fusion were driving factors in the selective

83 pressure that gave rise to new variants in the first half of the pandemic. New SARS-
84 CoV-2 variants displayed more enhanced cell fusogenicity and proteolytic efficiency
85 relative to earlier strains, starting with the first dominant spike mutation, D614G. Alpha
86 and Beta both showed significantly increased fusogenicity and Delta even more so
87 relative to them (17–21). However, this pattern ended with the rise of the Omicron
88 sublineages as they rely predominantly on endosomal-mediated entry and have
89 significantly reduced fusogenicity (22–26).
90
91 Virus-specific mutations are not the only determinant of viral entry and pathogenicity, as
92 various host genotypes can affect virus-host interactions. SNPs in TMPRSS2 and ACE2
93 for example have been associated with differential COVID-19 risk and/or severity (27–
94 31). Extensive research has been conducted better elucidate the determinants of
95 SARS-CoV-2 pathogenicity. In this study, we investigated the cause of an unexpected
96 inhibition of viral entry by serum samples from patients not previously exposed to
97 SARS-CoV-2. We identify the likely causative factor and discuss its potential role within
98 a complex system where proteases, antiproteases, host genomics, and viral genomics
99 interact and influence each other.
100

101 **RESULTS**

102

103 **Serum inhibition of protease-mediated entry of SARS-CoV-2 pseudoparticles and**
104 **live virus**

105 SARS-CoV-2 entry is efficiently mediated by a host of endogenous, exogenous, and cell
106 surface proteases. Assays investigating viral entry and entry inhibition should faithfully
107 recapitulate proteolytic activation (Figure 1A) for optimal physiological relevance. Using
108 VSVΔG pseudotyped particles bearing SARS-CoV-2 spike (CoV2pp) we have shown
109 that we can optimize entry efficiency by treatment with exogenous trypsin and followed
110 by treatment with soybean trypsin inhibitor to limit cytotoxicity (32). We tested our
111 trypsin-treated CoV2pp for validity using human serum samples, careful to only using
112 pre-pandemic samples as negative controls (Supplementary Figure 1A-B) (32). As
113 anticipated, sera from SARS-CoV-2 antibody-positive patients exhibit significantly
114 stronger neutralization compared to seronegative sera (Figure 1B-C and Supplementary
115 Figure 1C-F).

116

117 Unexpectedly, we found that sera from SARS-CoV-2 naïve patients were also capable
118 of neutralizing these pseudoviruses despite negative Spike ELISA results
119 (Supplementary Figure 1A). An external group at Louisiana State University Health
120 Shreveport (LSUHS) confirmed these findings using the same CoV2pp assay and
121 experimental conditions (Figure 1C and Supplementary Figure 1B, C-F). In both groups,
122 SARS-CoV-2 naïve sera inhibited CoV2pp entry by 90-97% (Supplementary Figure 1E,
123 F). However, seropositive patient sera exhibited inhibition orders of magnitude beyond

124 this threshold, suggesting antibody mediated inhibition of CoV2pp entry (Figure 1C and
125 Supplementary Figure 1C-F). Additionally, using identical serum samples as LSUHS,
126 collaborators at the University of Texas Medical Branch at Galveston (UTMB) also
127 observed significant neutralization of authentic SARS-CoV-2 by seronegative sera, as
128 assayed by a plaque reduction neutralization assay (PRNT) (Fig. 1E and Supplemental
129 Fig. 1G).
130
131 During the validation and optimization our CoV2pp system, we described that this
132 inhibition was abolished by heat-inactivation at 56ºC for 1hr (32). Here we show a
133 schematic representing entry inhibition by naïve sera from our previously published
134 findings and replicated by other published SARS-CoV-2 neutralization assays using
135 proteolytic activation without sufficient heat inactivation (33–35) (Figure 1B). These
136 findings imply the existence of a heat-labile serum factor or factors capable of inhibiting
137 protease-mediated entry of SARS-CoV-2.
138
139 **A serum factor capable of inhibiting protease-mediated entry**
140 Upon observing and verifying our results, we identified alpha-1-antitrypsin (AAT) and
141 alpha-2-macroglobulin (A2M) as abundant and heat labile products in serum that may
142 be responsible for inhibition of protease-mediated entry (36–39). These blood products
143 are typically present in human serum at high concentrations—1.1-2.2 mg/mL for AAT
144 and 2-4 mg/mL for A2M—and have been described to inhibit both exogenous and
145 endogenous proteases (40). A2M and AAT alone are responsible for approximately
146 10% and 90% of serum antiprotease capacity, respectively (41).

147

148 In spite of the name, the primary physiological target of AAT is neutrophil elastase (NE),
149 a protease released by neutrophils and found at high concentrations during acute
150 inflammation, especially in the context of acute respiratory distress syndrome (ARDS)
151 secondary to COVID-19 (42–44). In order to lend weight to the AAT hypothesis, we
152 therefore investigated whether NE, like trypsin or TMPRSS2, was also capable of
153 enhancing CoV2pp entry. We found that NE potently enhances cellular entry relative to
154 untreated particles (Figure 2A), further underlying the potential role of AAT in inhibiting
155 protease-mediate entry *in vivo*.

156

157 To assess whether AAT and/or A2M alone could inhibit protease-mediated CoV2pp
158 entry, we treated with each at the time of infection and observed dose-dependent entry
159 inhibition by both AAT and A2M, with IC50s of 14.47μg/mL and 54.20μg/mL,
160 respectively (Figure 2B), values that are 50-100-fold below their concentration in serum
161 and bronchoalveolar lavage (BAL) (36, 40, 45). Importantly, neither protein inhibited
162 VSV-Gpp, replicating the inhibitory effect of naïve serum (Figure 2C). Albumin, the most
163 abundant protein in blood, showed no significant reduction of entry of either CoV2pp or
164 VSV-Gpp (Figure 2B), underscoring that the inhibitory effects of AAT and A2M on
165 CoV2-S mediated entry was specific.

166

167 While these findings suggest that AAT—and to a lesser extent A2M—can inhibit
168 exogenous proteases known to enhance SARS-CoV-2 entry, SARS-CoV-2 infection is
169 also mediated by proteases at the cell surface as well as endosomal proteases (Figure

170 1A). TMPRSS2 and cathepsin L are well-characterized examples of cell surface and
171 endosomal proteases, respectively. AAT and A2M are secreted extracellular proteins
172 that can access the former but likely not the latter. Therefore, we sought to investigate
173 whether either protein could inhibit TMPRSS2-mediated SARS-CoV-2 entry. We first
174 showed that saturating amounts of nafamostat mesylate, a specific inhibitor of
175 TMPRSS2, maximally inhibited ~80% of CoV2pp entry in 293T-ACE2/TMPRSS2 cells
176 (Figure 3A) but had no effect on isogenic 293T-ACE2 cells (Figure 3B). This is
177 consistent with the use of endosomal proteases such as Cathepsin L in the absence of
178 TMPRSS2 or other exogenous proteases. Soluble Spike receptor binding domain
179 (sRBD) completely abolished CoV2pp entry in both cell lines confirming that entry was
180 still entirely ACE2-dependent (Figure 3A-B).
181
182 To examine inhibition of TMPRSS2-mediated entry by AAT and A2M, we infected both
183 cell lines with non-protease-treated CoV2pp. We observed that AAT inhibited CoV2pp
184 entry into 293T-ACE/TMPRSS2 cells, but not 293T-ACE2 cells (Figure 3C, D). A2M and
185 albumin both displayed no entry inhibition at the concentrations tested. AAT inhibition of
186 entry into the 293T ACE2-TMPRSS2 cells resulted in approximately a 70% drop in
187 relative infection (Figure 3C). This finding indicates that AAT inhibition accounts for
188 much of the entry attributed to TMPRSS2 enhancement, given that the use of
189 nafamostat mesylate resulted in a maximal inhibition of 80% in the 293T ACE2-
190 TMPRSS2 cells (Figure 3A). This observation suggests that AAT plays a significant role
191 in inhibiting TMPRSS2-mediated entry even at concentrations far below those seen in
192 serum and bronchioalveolar lavage (BAL) (1.1 – 2.2 milligrams/ml) (36, 40, 45).

193

194 In summary, our findings provide evidence that AAT, and to a lesser extent A2M, can
195 inhibit protease-mediated entry of SARS-CoV-2 in a cell culture model. AAT
196 demonstrated the ability to inhibit not only exogenous proteases like trypsin but also cell
197 surface protease TMPRSS2, which plays a crucial role in SARS-CoV-2 entry. These
198 results highlight the potential role of these serum factors in modulating viral entry *in*
199 *vivo*.

200

201 **AAT inhibits protease-mediated entry of authentic SARS-CoV-2**

202 To test whether these findings held for authentic SARS-CoV-2, we infected 293T-ACE2
203 cells and treated them with elastase, trypsin, or a cathepsin inhibitor (E64). We
204 measured the fraction of cells infected with SARS-CoV-2 at 6, 12, 24, and 36 hours
205 post-infection. Consistent with our CoV2pp observations, both elastase and trypsin
206 significantly enhanced entry, while E64 inhibited infection as expected, by inhibiting the
207 cathepsin-mediated pathway utilized when exogenous proteases and TMPRSS2 are
208 absent (Figure 4A).

209

210 Next, we performed serial dilutions of AAT in the presence of trypsin- and elastase-
211 treated SARS-CoV-2 at 24 hours post-infection (Figure 4B,C). We observed a dose-
212 dependent inhibition of protease-mediated entry, with potent inhibition at concentrations
213 far below those present in serum and bronchoalveolar lavage fluid. These results are
214 consistent with those obtained using the CoV2pp system, further demonstrating that
215 AAT can inhibit protease-mediated entry of live SARS-CoV-2.

216

217 In conclusion, our experiments with authentic SARS-CoV-2 validate the findings
218 obtained using the CoV2pp system, showing that AAT can effectively inhibit protease-
219 mediated entry of the virus. This highlights the potential physiological relevance of AAT
220 in modulating SARS-CoV-2 infection.

221

222 **Serum-inhibition of rVSVCov2 entry is reduced in subjects with AAT deficient**
223 **genotypes**

224 Recognizing AATs potential as an inhibitor of protease-mediated entry enhancement,
225 we aimed to better elucidate the potential physiological relevance of these findings to
226 individuals of various AAT genotypes. AAT levels in serum varies across individuals and
227 are determined by co-dominant alleles in the SERPINA1 gene. The four genotypes
228 investigated here are designated as PI*MM, PI*MS, PI*MZ, and PI*ZZ. Typically, PI*MM
229 individuals have normal AAT levels, while PI*MS and PI*MZ individuals have varying
230 amounts that range from near to sub-normal AAT levels. PI*ZZ individuals are
231 considered AAT deficient (AATD) (Figure 5A).

232

233 To better elucidate the physiological implications our findings we obtained pre-2020
234 serum samples from individuals with these four major AAT genotypes and tested their
235 ability to inhibit SARS-CoV-2 Spike-mediated entry. We used replication-competent
236 VSV containing Spike in place of G (rVSV-CoV-2-S) to model SARS-CoV-2 entry. We
237 first infected Vero cells with trypsin-treated WT rVSV-CoV-2-S in the presence of
238 serially diluted serum from the indicated genotypes (Fig. 5B and Supplemental Figure

239 2A). At 12 hours post-infection, we observed elevated GFP expression at higher serum
240 concentrations for PI*ZZ samples compared to PI*MM, PI*MS, and PI*MZ samples
241 (Figure 5B and Supplemental Figure 2A). This suggests that the most severe AATD
242 genotypes have reduced serum inhibitory potential against protease-mediated entry of
243 WT SARS-CoV-2 Spike, but this reduction is not observed for heterozygotes of the Z
244 and S alleles.
245
246 During the SARS-CoV-2 pandemic, several viral lineages have emerged and become
247 dominant. While many similarities exist between all variants of concern (VOCs), some
248 show distinct differences, particularly in viral entry and proteolytic processing of Spike
249 (4, 22, 25). Therefore, we investigated whether the effects of AAT would remain
250 consistent across all SARS-CoV-2 VOCs.
251
252 Using our rVSV-CoV-2-S system, we compared entry of isogenic viruses differing only
253 in Spike to model entry by different SARS-CoV-2 VOCs (1). The pattern observed for
254 WT rVSV-CoV-2-S was also seen with Delta rVSV-CoV-2-S containing the Spike
255 protein from B.1.617.2. This VOC became dominant in mid to late 2021, and AATD sera
256 were still less able to inhibit protease-mediated entry (Figure 5C).
257
258 Finally, we examined Omicron rVSV-CoV2 containing the Spike protein from B.1.1.529.
259 The Omicron lineage became dominant in 2022 and has remained the dominant lineage
260 since (46), overtaking Delta as the primary VOC in circulation. Notably, Omicron has
261 been shown to undergo less enhancement of entry by proteolytic activation of Spike

262 (22, 25). Using Omicron rVSV-CoV2, we observed no significant difference in inhibitory
263 potential between PI*ZZ and other AAT genotypes (Figure 5D), unlike what we observe
264 for Delta and WT (Figure 5B,C). These data suggest that AAT, and consequently AATD,
265 may have less impact on protease-mediated entry for the Omicron variant compared to
266 WT and Delta variants.
267
268

DISCUSSION

In this study, we identify alpha-1 antitrypsin as the primary inhibitor of protease-mediated entry of SARS-CoV-2 in naïve serum. We demonstrated that AAT effectively inhibits entry mediated by trypsin, elastase, or TMPRSS2. Furthermore, we found that serum from individuals with at least one functional AAT allele (PI*MM, PI*MS, PI*MZ) can inhibit protease-mediated entry by both WT and Delta SARS-CoV-2. Notably, serum from subjects homozygous for AATD alleles (PI*ZZ) exhibited reduced ability to inhibit WT and Delta entry. However, genotype-dependent inhibition of entry was not observed for the Omicron variant, as all serum samples—regardless of subject genotype—displayed similar inhibitory potential. This finding highlights the potential for AAT's role to vary depending on the entry mechanisms predominantly relied on by the virus.

Approximately 116 million individuals worldwide carry AATD alleles—PI*S or PI*Z—and 3.4 million people are homozygous for AATD—PI*SS, PI*SZ, and PI*ZZ (47). In the early stages of the COVID-19 pandemic, studies reported correlations between mortality rates and the geographic distribution of AAT deficiency (48–50). More recent retrospective analyses indicate that heterozygotes for AATD alleles (e.g. PI*MS, PI*MZ) do not appear to face an increased risk of severe COVID-19 (51). This observation aligns with our findings regarding the inhibitory potential of PI*MM, PI*MS, and PI*MZ sera. Unfortunately, determining a clear increased risk of COVID-19 severity for PI*ZZ patients remains elusive, as large-scale population studies have not yet included a

292 sufficient number of these individuals (52–54). Moreover, disentangling the confounding
293 influence of patients' awareness of their AATD status presents a challenge. In Germany,
294 survey data from March 2021 revealed that individuals diagnosed with AATD were more
295 concerned with being infected, more likely to restrict their social groups in response,
296 and saw a 65% drop in the percent who had been infected relative to the general
297 population (55).
298
299 An additional contributing factor in elucidating the risk associated the alpha-1 antitrypsin
300 deficiency is the emergence of the Omicron lineage of SARS-CoV-2, which is less
301 dependent on the protease-mediated entry pathway for efficient infection (25). As
302 Omicron has become the dominant variant, it has affected the potential risk factors for
303 more severe COVID-19. New variants may alter the role of AAT in disease severity,
304 leading to a different risk profile for individuals with AATD. The COVID-AATD Study
305 from Spain, involving over 2000 patients, showed that both AATD mutations and AAT
306 serum concentration below 116 mg/dl were associated with severe COVID-19 (56). One
307 limitation of this study might be that it was conducted from 1 May 2021 to 1 September
308 2022, and Omicron (BA.1) overtook Delta as the dominant strain in Spain around 3
309 January 2022 (57). If AATs antiprotease activity is playing a significant role in their
310 findings of increased risk of COVID-19 severity, separating subjects by estimated date
311 of infection may uncover whether the relationship is lessened after January 2022.
312
313 AAT has been predominantly described in the SARS-CoV-2 literature for its role as an
314 acute phase protein in modulating the host immune response (58). AAT plays a critical

315 part in modulating inflammation by inhibiting elastase and other factors (59–62). It is
316 involved in the formation of neutrophil extracellular traps (NETs) in acute pneumonia
317 and can modulate activities resulting in downstream IL-6 inhibition, which is heavily
318 implicated in COVID-19 pathogenicity (41–44, 63). In particular, the IL-6:AAT ratio is
319 highly correlated with COVID-19 severity (64). AAT is also noted for its regulatory role in
320 the coagulation cascade which may have relevance in preventing COVID-19
321 thromboses (43, 65–67). Previous works have also noted the importance of AAT's
322 ability to inhibit TMPRSS2 (68). Our study further elucidates the antiprotease role of
323 AAT and suggests that the presence or absence of functional AAT could influence the
324 efficiency of viral entry in other respiratory pathogens.
325
326 Patients diagnosed with AATD can receive supplementation through an FDA approved
327 medication: either IV or aerosolized AAT. Four clinical trials for use of AAT in the
328 context of COVID-19 have been registered. One never proceeded beyond recruitment
329 (NCT04385836), one was completed but has not published results (NCT04495101),
330 and one was stopped for futility (NCT04547140). One focused on treating with AAT
331 following a diagnosis of Acute Respiratory Distress Syndrome (ARDS) and saw
332 moderate effects, mostly on modulating inflammation (EudraCT 2020-001391-15) (69).
333 AAT as a treatment for proteolytically activated respiratory viruses shows promise as
334 both an immune modulator as well as a protease-inhibitor and would be well served by
335 clinical trials investigating treatment of a larger patient population as well as treatment in
336 the earlier stages of infection.
337

338 Despite the modest results seen in clinical trials of AAT supplementation, the clinical
339 implications of these findings for patients with an AAT deficiency are significant. Typical
340 clinical guidance is that AATD patients are only at increased risk of respiratory
341 infections secondary to chronic obstructive pulmonary disease, not primarily due to the
342 lack of functional AAT except in the case of immune dysregulation (70, 71). Our work
343 suggests this may miss the AATs role as an inhibitor of serine proteases and how that
344 might affect respiratory pathogens reliant on proteolytic activation. For example, not
345 only is TMPRSS2 known to be an important protease for proteolytic activation of the
346 surface glycoprotein hemagglutinin in H1, H3, H7, and H10 influenza A viruses (IAV)
347 (72, 73) but AAT specifically has been shown to inhibit protease-mediated entry of
348 H3N2 IAV and influenza B virus (72). Additionally, multiple studies have implicated AAT
349 in HIV entry as well (62, 74, 75). AAT's role in viral entry may be specific to the reliance
350 on proteolytic processing at or outside the cell. We show that in the case of SARS-CoV-
351 2, new variants may alter that role, leading to a different risk profile for individuals with
352 AATD. It is crucial to continue investigating the relationship between AAT and new
353 variants to better understand the evolving landscape of risk factors for COVID-19.
354 Furthermore, our findings suggest that it may be worthwhile to invest more into
355 investigating the role of AAT in other respiratory viruses mediated by serine proteases
356 (76, 77). A better understanding of the interplay between AAT and these viruses could
357 help identify potential therapeutic targets, improve patient outcomes, and affect clinical
358 guidance for AATD patients in relation to other respiratory pathogens.
359

360 In conclusion, our study highlights the critical role of AAT in inhibiting protease-mediated
361 entry of SARS-CoV-2 and its potential implications for treatment, especially in patients
362 with AAT deficiency. As the COVID-19 pandemic evolves with the emergence of new
363 variants, understanding the role of AAT in the context of these variants is crucial for
364 assessing the shifting risk profiles of individuals with AATD. Our findings also suggest
365 that AAT may play a role in the pathogenesis of other respiratory viruses mediated by
366 serine proteases, opening avenues for future research into the therapeutic potential of
367 AAT in treating these infections. Investigating the role of AAT in other respiratory
368 viruses could lead to the identification of potential therapeutic targets, improved patient
369 outcomes, and updated clinical guidance for AATD patients in relation to other
370 respiratory pathogens. Lastly, further investigation is needed to expand our
371 understanding of AAT's clinical implications, including the efficacy of AAT
372 supplementation for treating respiratory infections and determining the risk factors for
373 AATD patients in the context of COVID-19 and other respiratory illnesses. By deepening
374 our understanding of AAT's role in viral pathogenicity and its potential as a therapeutic
375 target, we can better inform clinical practice and contribute to improved public health
376 outcomes.

377 **METHODS**

378 Maintenance and generation of isogenic cell lines:

379 Vero-CCL81, BHK-21, Bsr-T7 (78), 293T, 293T ACE2, and 293T ACE2-TMPRSS2 cells
380 were cultured in DMEM with 10% heat inactivated FBS at 37ºC in the presence of 5%
381 CO2. Isogenic 293T ACE2, and 293T ACE2-TMPRSS2 cell clones were generated by
382 lentivirus transduction to stably express ACE2 only or ACE2 and TMPRSS2. ACE2
383 expression was under puromycin selection and TMPRSS2 was under blasticidin
384 selection as previously described (32).

385

386 Production of VSVΔG pseudotyped particles and neutralization studies:

387 Detailed protocols for the production and use of standardized VSVpp (CoV2pp and
388 VSV-Gpp) are given in Oguntuyo and Stevens et al (32). Briefly, 293T producer cells
389 were transfected to express the viral surface glycoprotein of interest, infected with
390 VSVΔG-rLuc-G* reporter virus, then virus supernatant collected and clarified 2 days
391 post infection prior to use. Trypsin-treated CoV2pp were treated as previously described
392 (32). All pseudotyped viruses were aliquoted prior to storage at -80ºC and tittered prior
393 to usage for neutralization experiments. Neutralization experiments were performed by
394 diluting the appropriate pseudotyped virus with a 4-fold serial dilution of Albumin
395 (Sigma-Aldrich, A8763), alpha-1-antitrypsin (Sigma-Aldrich, SRP6312), alpha-2-
396 macroglobulin (Sigma-Aldrich, SRP6314) or Nafamostat mesylate (Selleckchem,
397 S1386). SARS-CoV-2 soluble RBD (sRBD) with human IgG-Fc was produced using a
398 recombinant Sendai virus expression platform further described below. All infections

399 were processed for detection of Renilla luciferase activity at 20hrs post-infection, and
400 luminescence was read on the Cytation3 (BioTek).
401
402 SARS-CoV-2 plaque reduction neutralization titration (PRNT) by sera:
403 Neutralization experiments with live virus were performed by incubating sera with 50-
404 100 PFU of SARS-CoV-2, isolate USA-WA1/2020 P4, for one hour at 37ºC. All sera
405 were diluted in serum free DMEM. Serial dilutions started at a four-fold dilution and went
406 through seven three-fold serial dilutions. The virus-serum mixture was then used to
407 inoculate Vero E6 cells for one hour at 37ºC and 5% CO_2. Cells were overlaid with
408 EMEM medium (no FBS) and 1.25% Avicel, incubated for 3 days, and plaques were
409 counted after staining with 1% crystal violet in formalin.
410
411 SARS-CoV-2 infection of 293T-ACE2 cells and protease treatment:
412 SARS-CoV-2 isolate USA-WA1/2020 (NR-52281) was provided by the Center for
413 Disease Control and Prevention and obtained through BEI Resources, NIAID, NIH.
414 $1x10^6$ 293T cells stably transduced to express ACE2 were plated in a 6 well dish and
415 infected at an MOI of 0.01 for the time period indicated. Just before infection, virus was
416 treated with alpha-1-antitrypsin (Sigma-Aldrich, SRP6312) at the concentration noted,
417 elastase from human leukocytes (Sigma-Aldrich, E8140) at 0.167 mg/mL, TPCK-treated
418 trypsin (Sigma-Aldrich, T1426-1G) at 50 µg/mL, or E-64 (Sigma-Aldrich, E3132) at 100
419 µM. Cells were harvested into 4% PFA and were allowed to fix for 30 minutes prior to
420 staining for flow cytometry. Infection was determined with mouse anti-SARS-CoV
421 nucleoprotein antibody, directly conjugated to Alexa Fluor 594. Samples were collected

422 on through an Attune NxT Flow Cytometer and data was analyzed using FlowJo
423 software (v10.6.2). All SARS-CoV-2 work was performed in the CDC and USDA-
424 approved BSL-3 facility at the Icahn School of Medicine at Mount Sinai in accordance
425 with institutional biosafety requirements.
426
427 Production of Replication competent VSVΔG with SARS-CoV-2 Spike Variants and
428 Neutralization Studies:
429 VSV-eGFP was cloned into the pEMC vector containing an optimized T7 promotor and
430 hammerhead ribozyme. Original VSV-eGFP sequence was from pVSV-eGFP; a gift
431 from Dr. John Rose (79). pEMC-VSV-eGFP-CoV2 Spike was cloned as follows: human
432 codon optimized SARS-CoV-2 Spike variants with the 21 amino acid truncation of the
433 cytoplasmic tail were inserted into the VSV-G open reading frame (80) (rVSV-CoV2).
434 The Spike transcriptional unit is flanked by MluI and PacI restriction sites. Expression
435 plasmids containing VSV N, P, M, G, and L open reading frames were each cloned into
436 a pCI vector backbone to allow for efficient virus rescue, generating pCI-VSV-N, pCI-
437 VSV-P, pCI-VSV-M, pCI-VSV-G, and pCI-VSV-L.
438
439 rVSV-CoV2 was rescued in $4x10^5$ 293T ACE2-TMPRSS2 or BHK-21 ACE2 cells (32) in
440 each well of a 6-well plate. 2000 ng of pEMC-VSV-EGFP-CoV2 spike, 2500 ng of
441 pCAGGS-T7opt (81), 850 ng of pCI-VSV-N, 400 ng of pCI-VSV-P, 100 ug of pCI-VSV-
442 M, 100 ng of pCI-VSV-G, 100 ng of pCI-VSV-L were mixed with 4 ml of Plus reagent
443 and 6.6 ml of Lipofectamine LTX (Invitrogen). 30 minutes later, the transfection mixture
444 was applied to 293T ACE2-TMPRSS2 cells dropwise. Cells were maintained with

445 medium replacement every day for 4-5 days until GFP positive syncytia appeared.
446 Rescued viruses were amplified in VeroCCL81 TMPRSS2 cells (32), harvested after 6
447 days, stored at -80C. For titration, $5x10^4$ 293T ACE2-TMPRSS2 cells were seeded onto
448 each well of a 96-well plate and 24 hours later were infected with serially diluted rVSV-
449 CoV2 stock. Virus titer (IU/mL) was calculated 10 hours later by counting GFP positive
450 cells on the Celigo imaging cytometer (Nexcelom).
451
452 Human Sera Samples:
453 All patient sera were acquired after approval by the respective institutional review
454 boards (IRBs) and/or equivalent oversight bodies (Bioethics Committee, Independent
455 Ethics Committee), as follows: (i) the Mount Sinai Hospital IRB (New York, NY, USA),
456 (ii) the Louisiana State University Health Sciences Center—Shreveport (LSUHS, LA,
457 USA), and (iii) the Alpha-1 Foundation (University of Florida, Coral Gables, FL, USA).
458 Samples were deidentified at the source institutions or by the respective principal
459 investigators (PIs) of the IRB-approved protocols for sample collection before analyses
460 performed in this study. All necessary patient/participant consent has been obtained,
461 and the appropriate institutional forms have been archived. Specifically, SERPINA1
462 genotyped sera samples collected before 2019 were obtained from the Alpha-1
463 Foundation.
464
465 Enzyme-Linked Immunosorbent Assay:
466 Spike ELISAs for patient sera from the Krammer lab were performed in a clinical setting
467 using the two-step protocol previously published (32, 82). Briefly, this involves screening

468 patient sera (at a 1:50 dilution) with the sRBD; samples determined to be positive were
469 further screened at 5 dilutions for reactivity to the spike ectodomain. Background was
470 subtracted from the OD values, samples were determined to be positive if their ODs
471 were ≥3-fold over that of the negative control, and the AUC was calculated in PRISM.
472 ELISAs performed by the LSUHS group utilized the sRBD with a 1:50 dilution of patient
473 serum to screen all samples, followed by use of the spike ectodomain with patient sera
474 at a 1:100 dilution. Background-subtracted OD values are reported for both sets of
475 ELISAs.
476
477 Production of Soluble SARS-CoV-2 Spike Receptor Binding Domain (sRBD):
478 Sendai virus (SeV) Z strain (AB855655.1) was cloned into a pRS vector backbone with
479 an additional eGFP transcriptional unit upstream of N. The F transcriptional unit was
480 derived from the SeV Fushimi strain (KY295909.1). We then generated an additional
481 transcriptional unit between the P gene and M gene. SARS-CoV-2 Spike receptor
482 binding domain (sRBD), amino acids 319-541, was taken from human codon optimized
483 Spike (MN908947) in a pCAGGS backbone, a gift from Dr. Florian Krammer (82), and
484 was fused to human IgG1 Fc (amino acids 220-449 of P0DOX5.2) at the C-terminus
485 (SeV-Z-eGFP-sRBD).
486
487 $2x10^5$ Bsr-T7 cells, stably expressing T7-polymerase, were seeded in a 6-well plate. 24
488 hours later 4 µg of pRS-SeV-Z-eGFP-sRBD, 4 µg of pCAGGS-T7opt, 1.44 µg of SeV-N,
489 0.77 µg of SeV-P, 0.07 µg of SeV-L were mixed with 5.5 µl of Plus reagent and 8.9 µl of
490 Lipofectamine LTX (Invitrogen). 30 minutes later, the transfection mixture was applied to

491 Bsr-T7 cells dropwise. Medium was replaced with DMEM + 0.2 µg /ml of TPCK-trypsin
492 (Millipore Sigma, #T1426) at one day post transfection, followed by media replacement
493 every day until infection reached confluency. Supernatant was stored at -80C.
494
495 Amplification was performed by seeding $5x10^6$ cells in a T175cm^2-flask one day before
496 infection. Cells were infected by SeV-Z-eGFP-sRBD at an MOI of 0.01 for one hour,
497 followed by a media replacement with 0.2 mg/ml of TPCK-trypsin-containing DMEM.
498 Cells were maintained with medium replacement by the same every day until infection
499 reached confluency. At maximal infection the medium was changed and replaced with
500 plain DMEM. Cells were incubated for additional 24 hours to allow for maximum protein
501 production. Supernatant was collected and centrifuged at 360 g for 5 minutes, then
502 filtered with 0.1 µm filter (Corning 500 mL Vacuum Filter/Storage Bottle System, 0.1 µm
503 Pore). The flow-through was then applied to a Protein G Sepharose (Millipore Sigma,
504 #GE17-0618-01) containing column (5ml polypropylene columns; ThermoFisher,
505 #29922), followed by wash and elution.
506
507 <u>Statistics and reproducibility:</u>
508 All statistical tests were performed using GraphPad Prism 9 software (La Jolla, CA).
509 For all figures, error bars represent standard deviation of the mean. Sample size and
510 replicates for each experiment are indicated in the figure legends. Technical replicates
511 were prepared in parallel within one experiment, and experimental replicates were
512 performed on separate days. Statistical comparisons as noted in figure legends.
513

ACKNOWLEDGMENTS

The authors acknowledge the following funding: KYO and CS were supported by Viral-Host Pathogenesis Training Grant T32 AI07647; KYO was additionally supported by F31 AI154739. BL acknowledges flexible funding support from NIH grants R01 AI123449, R21 AI1498033, and the Department of Microbiology and the Ward-Coleman estate for endowing the Ward-Coleman Chairs at the ISMMS. JPK and SSI acknowledge funding from a LSUHS COVID-19 intramural grant. JPK and SSI acknowledge additional funding from NIH grants AI116851 and AI143839, respectively. Figures created with BioRender.com. We thank Randy A. Albrecht for oversight of the conventional BSL3 biocontainment facility. We would also like to acknowledge the Alpha-1 Foundation and the University of Florida which kindly provided serum samples from SERPINA1-genotyped patients. BL wishes to dedicate this paper to Ernest L Robles-Levroney, the first graduate student BL had the privilege to train. Ernie Robles-Levroney was dedicated teacher, role model and trailblazer who passed away unexpectedly during the course of writing this manuscript.

530 **FIGURES**

531

532 **Figure 1. Overview of SARS-CoV-2 entry and inhibition of trypsin treated CoV2pp**
533 **entry by COVID-19 seronegative sera**. **(A)** Overview of SARS-CoV-2 entry. Two
534 modes of entry are displayed: 1) Entry mediated by endosomal proteases such as
535 Cathepsin B/L (late entry) and 2) protease-mediated entry (early entry), driven by cell-
536 surface proteases like TMPRSS2 and extracellular proteases such as trypsin and
537 elastase. Protease-mediated entry may be inhibited by the presence of antiproteases.
538 This model was created in Biorender. **(B)** A representative schematic of entry inhibition
539 of trypsin-treated SARS-CoV-2 pseudotyped particles (CoV2pp) by sera from COVID-19
540 recovered or naïve individuals (COVID sero (+) and COVID sero (-) sera, respectively).
541 This is a representation of results previously presented in supplemental Figure 3A of
542 Oguntuyo and Stevens et al, mBio 2021, as well as Figure 5B of Nie et al, 2020. Here,
543 sera samples were incubated with trypsin-treated CoV2pp prior to infection of Vero-
544 CCL81 cells. Grey lines represent seronegative sera and purple lines are COVID-19
545 seropositive sera. The dashed lines are samples that were heat inactivated (HI) prior to
546 use. **(C)** Seronegative and seropositive samples were first identified based on IgG
547 antibodies against Spike (Supplemental Figure 1B). Normalized infection data at the
548 highest and lowest dilutions tested are shown as % maximal infection (media only) with
549 results from seronegative plotted on log scale. Data points represent the mean of
550 neutralizations performed in quadruplicate with SEM bars, each line indicating a sample
551 from a unique donor. Maximal sera inhibition was compared using Welch's t test. **(D)**
552 SARS-CoV-2 seronegative sera do not inhibit VSV-Gpp. Four serum samples were

553 analyzed each in technical triplicate, means with SEM error bars shown. **(E)** Authentic
554 SARS-CoV-2 is modestly inhibited by seronegative sera. Sera samples also presented
555 in Supplementary Figure 1E were utilized for plaque reduction neutralization
556 experiments (PRNT) with live virus. Presented here are the mean of one experiment
557 done in technical duplicates with SEM error bars. Maximal sera inhibition was compared
558 using Welch's t test. (ns, not significant; **, $p < 0.01$; ***, $p < 0.005$, and ****, $p <$
559 0.0001).
560
561 **Figure 2. CoV2pp is enhanced by elastase treatment and alpha-1-antitrypsin**
562 **(AAT) and alpha-2-macroglobulin (A2M) inhibit trypsin-mediated enhancement of**
563 **CoV2pp entry. (A)** Treatment of both CoV2pp and VSV-Gpp with elastase in serum-
564 free media. All points are means with SEM bars for samples performed in technical
565 triplicate. Red dotted line marks normalized maximal infection level (100%). **(B)** AAT
566 and A2M inhibit trypsin-mediated enhancement of CoV2pp. Trypsin-treated
567 pseudoparticles were diluted in serum free media, then used to infect Vero-CCL81 cells
568 in the presence of the indicated concentrations of albumin, AAT, or A2M. Data are from
569 two independent experiments and are presented as percent relative infection where
570 each concentration was normalized to the lowest concentration of the test reagent used.
571 **(C)** Performed identical to (B), AAT, A2M, and albumin have no effect on VSV-Gpp
572 entry.
573
574

575 **Figure 3. Alpha-1-antitrypsin (AAT) inhibits TMPRSS2 mediated enhancement of**
576 **CoV2pp entry. (A,B)** CoV2pp were mixed with a serial dilution of either Nafamostat or
577 sRBD prior to infection of isogenic cells stably expressing (A) ACE2 and TMPRSS2 or
578 **(B)** ACE2. **(C)** AAT inhibits TMPRSS2-mediated enhancement of CoV2pp entry.
579 CoV2pp not treated with trypsin were diluted in DMEM+10% FBS and utilized to infect
580 293T-ACE2+TMPRSS2 clonal in the presence of the indicated concentrations of A2M,
581 AAT, or Albumin. **(D)** CoV2pp, treated exactly as in **(C)**, were used to infect a 293T-
582 ACE2 clonal cell line. Presented here are the results of an experiment done in technical
583 triplicates. Error bars show SEM and data were fit using variable slope, 4-parameter
584 logistics regression curve (robust fitting method). Significance calculated using a
585 Welch's T Test on the Area Under the Curve for each condition. (ns, not significant; **, p
586 < 0.01; ***, p < 0.005, and ****, p < 0.0001).
587
588 **Figure 4. Alpha-1-antitrypsin (AAT) inhibits protease-mediated enhancement of**
589 **authentic SARS-CoV-2 entry. (A)** Authentic SARS-CoV-2 entry in 293T-ACE2 clonal
590 cells over 36 hours under treatment of elastase, trypsin, E64, or untreated. Significance
591 calculated using a Welch's T Test on the Area Under the Curve for each condition. **(B)**
592 Authentic SARS-CoV-2 entry in 293T-ACE2 cells mediated by trypsin, treated by
593 increasing concentrations of AAT, collected at 0, 12, 24, or 36 hours post-infection. **(C)**
594 Authentic SARS-CoV-2 entry in 293T-ACE2 cells mediated by elastase, treated by
595 increasing concentrations of AAT. Data points are means +/- SEM from a representative
596 experiment performed in triplicate. (ns, not significant; **, p < 0.01; ***, p < 0.005, and
597 ****, p < 0.0001).

598

599

600 **Figure 5. rVSV-CoV2 entry inhibition by serum from subjects with variable AAT**
601 **genotypes. (A)** Expected range of concentrations of AAT in serum relative to AAT
602 genotype (data from Lopes et al (83)). **(B)** WT rVSV-CoV2 entry inhibition by serum
603 from 4 PI*MM subjects, 2 PI*MS subjects, 2 PI*MZ subjects, and 4 PI*ZZ subjects
604 performed in technical triplicate. Subject serum samples are identical for all data shown
605 across all variants. Boxes span 25-75th percentiles and median is noted. Whiskers span
606 minimum to maximum. **(C)** Delta rVSV-CoV2 entry inhibition by serum as described in
607 3B except only 2 PI*MM and 2 PI*ZZ subjects are shown. **(D)** Omicron rVSV-CoV2
608 entry inhibition by serum as described in 3B. All data shown performed in technical
609 triplicate. All rVSV-CoV-2 is trypsin-treated. Significance calculated using Welch's t test
610 (ns, not significant; **, $p < 0.01$; ***, $p < 0.005$, and ****, $p < 0.0001$).

611

612 **Supplemental Figure 1. Spike ELISA data and neutralization curves.** Spike
613 ectodomain ELISAs for **(A)** ISMMS or **(B)** LSUHS samples. Four seronegative and
614 seropositive samples were utilized. Shown are the OD490 values from the 1:100 sera
615 dilution with the median and interquartile range. **(C)** Seronegative and seropositive
616 samples were first identified based on IgG antibodies against Spike (Supplemental
617 Figure 1A). Normalized infection data at the highest and lowest dilutions tested are
618 shown as % maximal infection (media only) with results from seronegative plotted on
619 log scale. Data points represent the mean of neutralizations performed in quadruplicate
620 with SEM bars, each line indicating a sample from a unique donor. Maximal sera

621 inhibition was compared using Welch's t test. **(D)** Sera inhibition comparison against
622 VSV-Gpp for 4 sera samples collected at ISMMS. Sera inhibition comparisons for **(E)**
623 ISMMS or **(F)** LSUHS. Inhibition of trypsin treated CoV2pp entry by SARS-CoV-2
624 seropositive and seronegative sera independently observed. Collaborators in a different
625 state independently performed the identical experiment described in Fig. 1A with their
626 own cohort of seropositive and seronegative samples. Data shown are means from
627 technical quadruplicates/sample/dilution. Experiment performed and presented as in
628 Fig. 1C. **(G**) Live SARS-CoV-2 is inhibited by seropositive and seronegative sera. Sera
629 samples presented in Fig. 1C and (F) above were utilized for plaque reduction
630 neutralization experiments (PRNT) with live virus as described in the materials and
631 methods. Presented here are the mean of one experiment done in technical duplicates
632 and error bars show SEM. (ns, not significant; **, $p < 0.01$; ***, $p < 0.005$, and ****, $p <$
633 0.0001).
634
635 **Supplemental Figure 2.** Individual curves of rVSV-CoV2 entry inhibition by serum from
636 subjects with variable AAT genotypes in spike variants: **(A)** WT (Wuhan-Hu-1) and **(B)**
637 Omicron (B.1.1.529). Error bars show SEM and data were fit using variable slope, 4-
638 parameter logistics regression curve (robust fitting method). **(C)** Estimation plots for
639 area under the curve shown for PI*MM compared to PI*ZZ in WT rVSV-CoV2 and **(D)**
640 PI*MM compared to PI*ZZ in Omicron rVSV-CoV2. Significance calculated using a
641 Welch's t test on the Area Under the Curve for each condition. (ns, not significant; **, p
642 < 0.01; ***, $p < 0.005$, and ****, $p < 0.0001$).
643

644 **REFERENCES**

645 1. Stevens CS, Oguntuyo KY, Lee B. Proteases and variants: context matters for SARS-CoV-2
646 entry assays. *Curr. Opin. Virol.* 2021;50:49–58.

647 2. Hoffmann M et al. SARS-CoV-2 Cell Entry Depends on ACE2 and TMPRSS2 and Is Blocked
648 by a Clinically Proven Protease Inhibitor. *Cell* 2020;181(2):271-280.e8.

649 3. Zhu N et al. A Novel Coronavirus from Patients with Pneumonia in China, 2019. *N. Engl. J.*
650 *Med.* 2020;382(8):727–733.

651 4. Letko M, Marzi A, Munster V. Functional assessment of cell entry and receptor usage for
652 SARS-CoV-2 and other lineage B betacoronaviruses. *Nat. Microbiol.* 2020;5(4):562–569.

653 5. Tang T, Bidon M, Jaimes JA, Whittaker GR, Daniel S. Coronavirus membrane fusion
654 mechanism offers a potential target for antiviral development. *Antiviral Res.*
655 2020;178(March):104792.

656 6. Wrapp D et al. Cryo-EM structure of the 2019-nCoV spike in the prefusion conformation.
657 *Science* 2020;367(6483):1260–1263.

658 7. Zhu FC et al. Proteolytic activation of the SARS-coronavirus spike protein: Cutting enzymes
659 at the cutting edge of antiviral research. *J. Virol.* 2020;395(2):379–397.

660 8. Shang J et al. Cell entry mechanisms of SARS-CoV-2. *Proc. Natl. Acad. Sci.*
661 2020;117(21):11727–11734.

662 9. Tang T et al. Proteolytic Activation of SARS-CoV-2 Spike at the S1/S2 Boundary: Potential
663 Role of Proteases beyond Furin. *ACS Infect. Dis.* 2021;7(2):264–272.

664 10. Bhattacharyya C et al. SARS-CoV-2 mutation 614G creates an elastase cleavage site
665 enhancing its spread in high AAT-deficient regions. *Infect. Genet. Evol.* 2021;90:104760.

666 11. Belouzard S, Madu I, Whittaker GR. Elastase-mediated Activation of the Severe Acute
667 Respiratory Syndrome Coronavirus Spike Protein at Discrete Sites within the S2 Domain. *J.*
668 *Biol. Chem.* 2010;285(30):22758–22763.

669 12. Fuentes-Prior P. Priming of SARS-CoV-2 S protein by several membrane-bound serine
670 proteinases could explain enhanced viral infectivity and systemic COVID-19 infection. *J. Biol.*
671 *Chem.* 2021;296:100135.

672 13. Bollavaram K et al. Multiple sites on SARS-CoV-2 spike protein are susceptible to
673 proteolysis by cathepsins B, K, L, S, and V. *Protein Sci.* 2021;30(6):1131–1143.

674 14. B C et al. The spike glycoprotein of the new coronavirus 2019-nCoV contains a furin-like
675 cleavage site absent in CoV of the same clade [Internet]. *Antiviral Res.* 2020;176.
676 doi:10.1016/j.antiviral.2020.104742

677 15. G P et al. Furin cleavage of SARS-CoV-2 Spike promotes but is not essential for infection
678 and cell-cell fusion [Internet]. *PLoS Pathog.* 2021;17(1). doi:10.1371/journal.ppat.1009246

679 16. Peacock TP et al. The furin cleavage site in the SARS-CoV-2 spike protein is required for
680 transmission in ferrets. *Nat. Microbiol.* 2021;6(7):899–909.

681 17. Mlcochova P et al. SARS-CoV-2 B.1.617.2 Delta variant replication and immune evasion.
682 *Nature* 2021;599(7883):114–119.

683 18. Gobeil SM-C et al. D614G Mutation Alters SARS-CoV-2 Spike Conformation and Enhances
684 Protease Cleavage at the S1/S2 Junction. *Cell Rep.* 2021;34(2):108630.

685 19. Lubinski B et al. Spike Protein Cleavage-Activation in the Context of the SARS-CoV-2
686 P681R Mutation: an Analysis from Its First Appearance in Lineage A.23.1 Identified in Uganda.
687 *Microbiol. Spectr.* 2022;10(4):e01514-22.

688 20. Plante JA et al. Spike mutation D614G alters SARS-CoV-2 fitness. *Nature*
689 2021;592(7852):116–121.

690 21. Rajah MM et al. SARS-CoV-2 Alpha, Beta, and Delta variants display enhanced Spike-
691 mediated syncytia formation. *EMBO J.* 2021;40(24):e108944.

692 22. Zhao H et al. SARS-CoV-2 Omicron variant shows less efficient replication and fusion
693 activity when compared with Delta variant in TMPRSS2-expressed cells. *Emerg. Microbes*
694 *Infect.* 2022;11(1):277–283.

695 23. Hui KPY et al. SARS-CoV-2 Omicron variant replication in human bronchus and lung ex
696 vivo. *Nature* 2022;603(7902):715–720.

697 24. Meng B et al. Altered TMPRSS2 usage by SARS-CoV-2 Omicron impacts infectivity and
698 fusogenicity. *Nature* 2022;603(7902):706–714.

699 25. Willett BJ et al. SARS-CoV-2 Omicron is an immune escape variant with an altered cell
700 entry pathway. *Nat. Microbiol.* 2022;7(8):1161–1179.

701 26. Kumar S, Thambiraja TS, Karuppanan K, Subramaniam G. Omicron and Delta variant of
702 SARS-CoV-2: A comparative computational study of spike protein. *J. Med. Virol.*
703 2022;94(4):1641–1649.

704 27. Paniri A, Hosseini MM, Akhavan-Niaki H. First comprehensive computational analysis of
705 functional consequences of TMPRSS2 SNPs in susceptibility to SARS-CoV-2 among different
706 populations. *J. Biomol. Struct. Dyn.* 2021;39(10):3576–3593.

707 28. Jeon S et al. Regional TMPRSS2 V197M Allele Frequencies Are Correlated with COVID-19
708 Case Fatality Rates. *Mol. Cells* 2021;44(9):680–687.

709 29. Monticelli M et al. Protective Role of a TMPRSS2 Variant on Severe COVID-19 Outcome in
710 Young Males and Elderly Women. *Genes* 2021;12(4):596.

711 30. Li J et al. Polymorphisms and mutations of ACE2 and TMPRSS2 genes are associated with
712 COVID-19: a systematic review. *Eur. J. Med. Res.* 2022;27(1):26.

713 31. Schulert GS, Blum SA, Cron RQ. Host genetics of pediatric SARS-CoV-2 COVID-19 and
714 multisystem inflammatory syndrome in children. *Curr. Opin. Pediatr.* 2021;33(6):549.

715 32. Oguntuyo KY et al. Quantifying Absolute Neutralization Titers against SARS-CoV-2 by a
716 Standardized Virus Neutralization Assay Allows for Cross-Cohort Comparisons of COVID-19
717 Sera. *mBio* 2021;12(1):e02492-20.

718 33. Nie J et al. Establishment and validation of a pseudovirus neutralization assay for SARS-
719 CoV-2. *Emerg. Microbes Infect.* 2020;9(1):680–686.

720 34. Cruz-Cardenas JA et al. A pseudovirus-based platform to measure neutralizing antibodies in
721 Mexico using SARS-CoV-2 as proof-of-concept. *Sci. Rep.* 2022;12(1):17966.

722 35. Lam JH et al. Polymersomes as Stable Nanocarriers for a Highly Immunogenic and Durable
723 SARS-CoV-2 Spike Protein Subunit Vaccine. *ACS Nano* 2021;15(10):15754–15770.

724 36. Rehman AA, Ahsan H, Khan FH. Alpha-2-macroglobulin: A physiological guardian. *J. Cell.*
725 *Physiol.* 2013;228(8):1665–1675.

726 37. Blanco I. *Alpha-1 Antitrypsin Biology [Internet]*. Elsevier Inc.; 2017:

727 38. Bornhorst JA, Greene DN, Ashwood ER, Grenache DG. α1-Antitrypsin phenotypes and
728 associated serum protein concentrations in a large clinical population. *Chest* 2013;143(4):1000–
729 1008.

730 39. Sriram Vemuri, C. Tony Yu and NR. Formulation and Stability of Recombinant Alpha-1-
731 Antitrypsin [Internet]. In: Wang YJ, Pearlman R eds. *Stability and Characterization of Protein*
732 *and Peptide Drugs*. Boston, MA: Springer US; 1993:263–285

733 40. Strnad P, McElvaney NG, Lomas DA. Alpha 1 -Antitrypsin Deficiency. *N. Engl. J. Med.*
734 2020;382(15):1443–1455.

735 41. de Serres F, Blanco I. Role of alpha-1 antitrypsin in human health and disease. *J. Intern.*
736 *Med.* 2014;276(4):311–335.

737 42. Mohamed MMA, El-Shimy IA, Hadi MA. Neutrophil Elastase Inhibitors: A potential
738 prophylactic treatment option for SARS-CoV-2-induced respiratory complications?. *Crit. Care*
739 2020;24(1):311.

740 43. Middleton EA et al. Neutrophil Extracellular Traps (NETs) Contribute to Immunothrombosis
741 in COVID-19 Acute Respiratory Distress Syndrome [Internet]. *Blood* [published online ahead of
742 print: June 29, 2020]; doi:10.1182/blood.2020007008

743 44. Barnes BJ et al. Targeting potential drivers of COVID-19: Neutrophil extracellular traps
744 [Internet]. *J. Exp. Med.* 2020;217(6). doi:10.1084/jem.20200652

745 45. Olsen GN, Harris JO, Castle JR, Waldman RH, Karmgard HJ. Alpha-1-antitrypsin content in
746 the serum, alveolar macrophages, and alveolar lavage fluid of smoking and nonsmoking normal
747 subjects.. *J. Clin. Invest.* 1975;55(2):427–430.

748 46. Kirsebom FCM et al. COVID-19 vaccine effectiveness against the omicron (BA.2) variant in
749 England. *Lancet Infect. Dis.* 2022;22(7):931–933.

750 47. Greene CM et al. α1-Antitrypsin deficiency. *Nat. Rev. Dis. Primer* 2016;2(1):1–17.

751 48. Yoshikura H. Epidemiological correlation between COVID-19 epidemic and prevalence of
752 α-1 antitrypsin deficiency in the world. *Glob. Health Med.* 2021;3(2):73–81.

753 49. Shapira G, Shomron N, Gurwitz D. Ethnic differences in alpha-1 antitrypsin deficiency allele
754 frequencies may partially explain national differences in COVID-19 fatality rates. *FASEB J.*
755 2020;34(11):14160–14165.

756 50. Vianello A et al. Correlation between α1-Antitrypsin Deficiency and SARS-CoV-2 Infection:
757 Epidemiological Data and Pathogenetic Hypotheses. *J. Clin. Med.* 2021;10(19):4493.

758 51. Nygren D et al. Low Prevalence of Mild Alpha-1-Antitrypsin Deficiency in Hospitalized
759 COVID-19-Patients. *Int. J. Gen. Med.* 2022;Volume 15:5843–5848.

760 52. Faria N, Costa MI, Gomes J, Sucena M. Alpha-1 antitrypsin deficiency severity and the risk
761 of COVID-19: A Portuguese cohort [Internet]. *Respir. Med.* 2021;181.
762 doi:10.1016/j.rmed.2021.106387

763 53. Rodríguez-García C et al. Is SARS-COV-2 associated with alpha-1 antitrypsin deficiency?
764 [Internet]. *J. Thorac. Dis.* 2023;15(2). doi:10.21037/jtd-22-1062

765 54. Schneider CV, Strnad P. SARS-CoV-2 infection in alpha1-antitrypsin deficiency [Internet].
766 *Respir. Med.* 2021;184. doi:10.1016/j.rmed.2021.106466

767 55. Köhnlein T, Wilkens M, Eydt K. Auswirkungen der COVID-19-Pandemie auf das
768 Informationsmanagement und die Therapieadhärenz von substituierten Patienten mit Alpha-1-
769 Antitrypsin-Mangel (AATM). *Pneumologie* 2022;76(07):494–498.

770 56. Rodríguez Hermosa JL et al. Severe COVID-19 Illness and α1-Antitrypsin Deficiency:
771 COVID-AATD Study. *Biomedicines* 2023;11(2):516.

772 57. SARS-CoV-2 sequences by variant [Internet]. *Our World Data*
773 https://ourworldindata.org/grapher/covid-variants-bar. cited April 1, 2023

774 58. de Loyola MB et al. Alpha-1-antitrypsin: A possible host protective factor against Covid-19.
775 *Rev. Med. Virol.* 2021;31(2):e2157.

776 59. Zhou Z et al. Heightened Innate Immune Responses in the Respiratory Tract of COVID-19
777 Patients. *Cell Host Microbe* 2020;27(6):883-890.e2.

778 60. Lucas C et al. Longitudinal analyses reveal immunological misfiring in severe COVID-19
779 [Internet]. *Nature* [published online ahead of print: July 27, 2020]; doi:10.1038/s41586-020-
780 2588-y

781 61. Liao M et al. Single-cell landscape of bronchoalveolar immune cells in patients with
782 COVID-19. *Nat. Med.* 2020;26(6):842–844.

783 62. Bryan CL et al. HIV infection is associated with reduced serum alpha-1-antitrypsin
784 concentrations. *Clin. Investig. Med. Med. Clin. Exp.* 2010;33(6):E384-389.

785 63. Grifoni E et al. Interleukin-6 as prognosticator in patients with COVID-19 [Internet]. *J.*
786 *Infect.* [published online ahead of print: June 2020]; doi:10.1016/j.jinf.2020.06.008

787 64. McElvaney OJ et al. Characterization of the Inflammatory Response to Severe COVID-19
788 Illness. *Am. J. Respir. Crit. Care Med.* 2020;202(6):812–821.

789 65. Janciauskiene S, Welte T. Well-Known and Less Well-Known Functions of Alpha-1
790 Antitrypsin. Its Role in Chronic Obstructive Pulmonary Disease and Other Disease
791 Developments. *Ann. Am. Thorac. Soc.* 2016;13(Supplement_4):S280–S288.

792 66. Jose RJ, Manuel A. COVID-19 cytokine storm: the interplay between inflammation and
793 coagulation. *Lancet Respir. Med.* 2020;8(6):e46–e47.

794 67. Giannis D, Ziogas IA, Gianni P. Coagulation disorders in coronavirus infected patients:
795 COVID-19, SARS-CoV-1, MERS-CoV and lessons from the past [Internet]. *J. Clin. Virol.*
796 2020;127. doi:10.1016/j.jcv.2020.104362

797 68. Azouz NP et al. Alpha 1 Antitrypsin is an Inhibitor of the SARS-CoV-2–Priming Protease
798 TMPRSS2. *Pathog. Immun.* 2021;6(1):55–74.

799 69. McElvaney OJ et al. A randomized, double-blind, placebo-controlled trial of intravenous
800 alpha-1 antitrypsin for ARDS secondary to COVID-19. *Med* 2022;3(4):233-248.e6.

801 70. Meseeha M, Attia M. Alpha 1 Antitrypsin Deficiency [Internet]. In: *StatPearls*. Treasure
802 Island (FL): StatPearls Publishing; 2023:

803 71. Black L, Kueppers F. alpha1-Antitrypsin deficiency in nonsmokers.. *Am. Rev. Respir. Dis.*
804 1978;117(3):421–428.

805 72. Harbig A et al. Transcriptome profiling and protease inhibition experiments identify
806 proteases that activate H3N2 influenza A and influenza B viruses in murine airways. *J. Biol.*
807 *Chem.* 2020;295(33):11388–11407.

808 73. Böttcher-Friebertshäuser E et al. Cleavage of Influenza Virus Hemagglutinin by Airway
809 Proteases TMPRSS2 and HAT Differs in Subcellular Localization and Susceptibility to Protease
810 Inhibitors. *J. Virol.* 2010;84(11):5605–5614.

811 74. Potthoff AV, Münch J, Kirchhoff F, Brockmeyer NH. HIV infection in a patient with alpha-1
812 antitrypsin deficiency: a detrimental combination?. *AIDS Lond. Engl.* 2007;21(15):2115–2116.

813 75. Zhou X et al. Alpha-1-antitrypsin interacts with gp41 to block HIV-1 entry into CD4+ T
814 lymphocytes. *BMC Microbiol.* 2016;16(1):172.

815 76. Peitsch C, Klenk H-D, Garten W, Böttcher-Friebertshäuser E. Activation of Influenza A
816 Viruses by Host Proteases from Swine Airway Epithelium. *J. Virol.* 2014;88(1):282–291.

817 77. Hatesuer B et al. Tmprss2 Is Essential for Influenza H1N1 Virus Pathogenesis in Mice.
818 *PLOS Pathog.* 2013;9(12):e1003774.

819 78. Buchholz UJ, Finke S, Conzelmann KK. Generation of bovine respiratory syncytial virus
820 (BRSV) from cDNA: BRSV NS2 is not essential for virus replication in tissue culture, and the
821 human RSV leader region acts as a functional BRSV genome promoter. *J. Virol.*
822 1999;73(1):251–259.

823 79. Ramsburg E et al. A Vesicular Stomatitis Virus Recombinant Expressing Granulocyte-
824 Macrophage Colony-Stimulating Factor Induces Enhanced T-Cell Responses and Is Highly
825 Attenuated for Replication in Animals. *J. Virol.* 2005;79(24):15043–15053.

826 80. Case JB et al. Neutralizing Antibody and Soluble ACE2 Inhibition of a Replication-
827 Competent VSV-SARS-CoV-2 and a Clinical Isolate of SARS-CoV-2. *Cell Host Microbe*
828 2020;28(3):475-485.e5.

829 81. Beaty SM et al. Efficient and Robust Paramyxoviridae Reverse Genetics Systems. *mSphere*
830 2017;2(2):e00376-16.

831 82. Amanat F et al. A serological assay to detect SARS-CoV-2 seroconversion in humans. *Nat.*
832 *Med.* 2020;26(7):1033–1036.

833 83. Lopes AP et al. Portuguese consensus document for the management of alpha-1-antitrypsin
834 deficiency. *Pulmonology* 2018;24 Suppl 1:1–21.

835

Alpha-1-antitrypsin and its variant-dependent role in COVID-19 pathogenesis

Christian S Stevens[1#], Kasopefoluwa Y Oguntuyo[1#], Shreyas Kowdle[1], Luca Brambilla[1], Griffin Haas[1], Aditya Gowlikar[1], Mohammed NA Siddiquey[2], Robert M Schilke[2], Matthew D Woolard[2], Hongbo Zhang[2], Joshua A Acklin[1], Satoshi Ikegame[1], Chuan-Tien Huang[1], Jean K Lim[1], Robert W Cross[3], Thomas W Geisbert[3], Stanimir S Ivanov[2], Jeremy P Kamil[2], the Alpha-1 Foundation[4], and Benhur Lee[1]

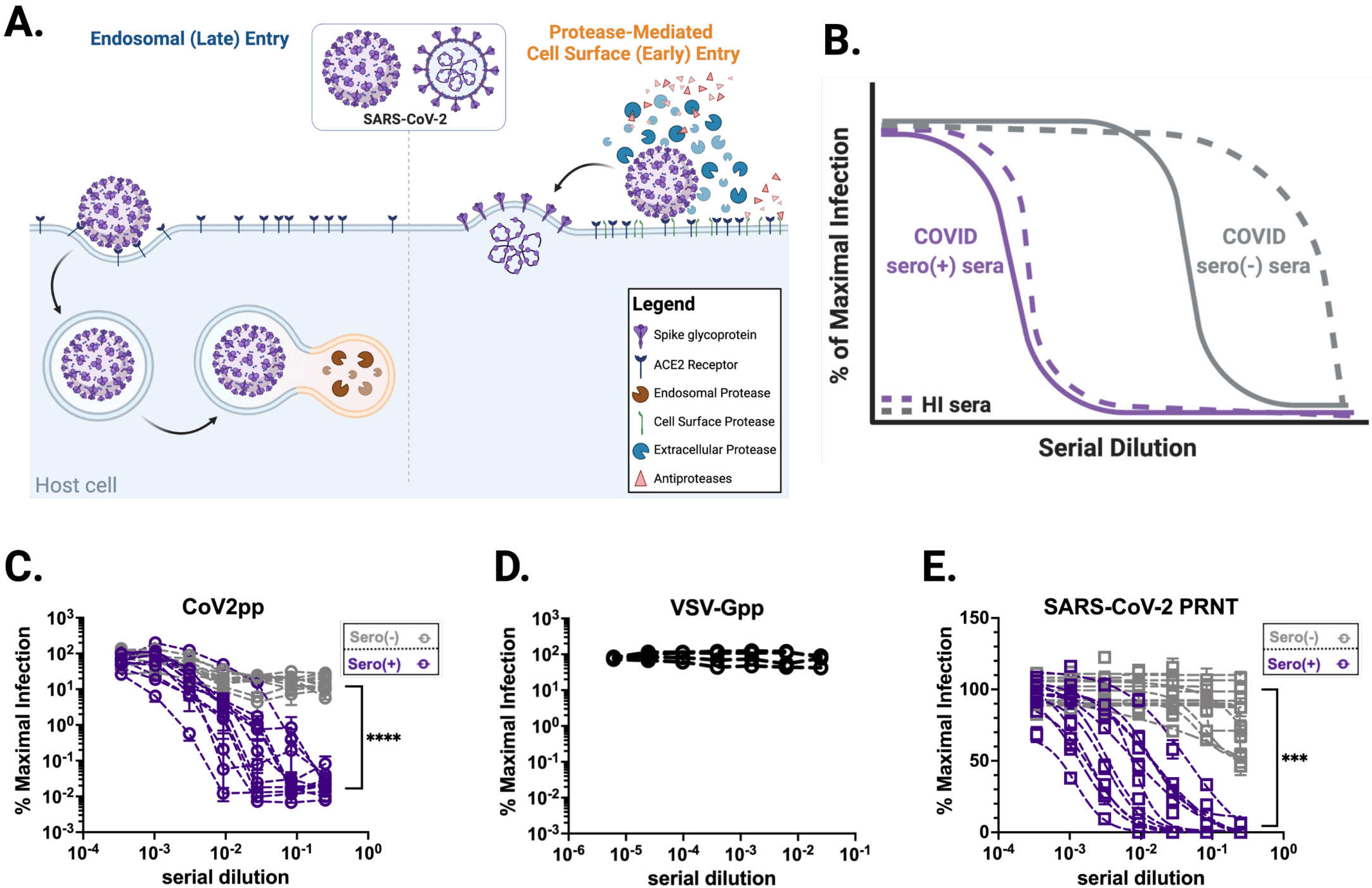
A.
Endosomal (Late) Entry
SARS-CoV-2
Protease-Mediated
Cell Surface (Early) Entry
Host cell
Legend
Spike glycoprotein
ACE2 Receptor
Endosomal Protease
Cell Surface Protease
Extracellular Protease
Antiproteases
B.
% of Maximal Infection
COVID
sero(+) sera
COVID
sero(-) sera
HI sera
Serial Dilution
C.
CoV2pp
Sero(-)
Sero(+)
****
% Maximal Infection
serial dilution
D.
VSV-Gpp
% Maximal Infection
serial dilution
E.
SARS-CoV-2 PRNT
Sero(-)
Sero(+)
***
% Maximal Infection
serial dilution

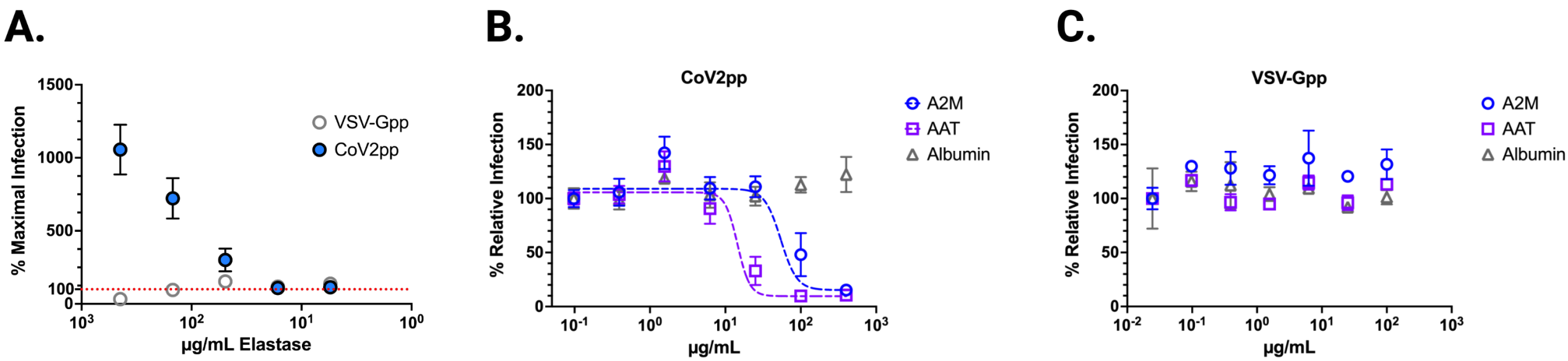
A.
% Maximal Infection
1500
1000
500
100
0
VSV-Gpp
CoV2pp
10^3
10^2
10^1
10^0
µg/mL Elastase
B.
CoV2pp
% Relative Infection
200
150
100
50
0
A2M
AAT
Albumin
10^{-1}
10^0
10^1
10^2
10^3
µg/mL
C.
VSV-Gpp
% Relative Infection
200
150
100
50
0
A2M
AAT
Albumin
10^{-2}
10^{-1}
10^0
10^1
10^2
10^3
µg/mL

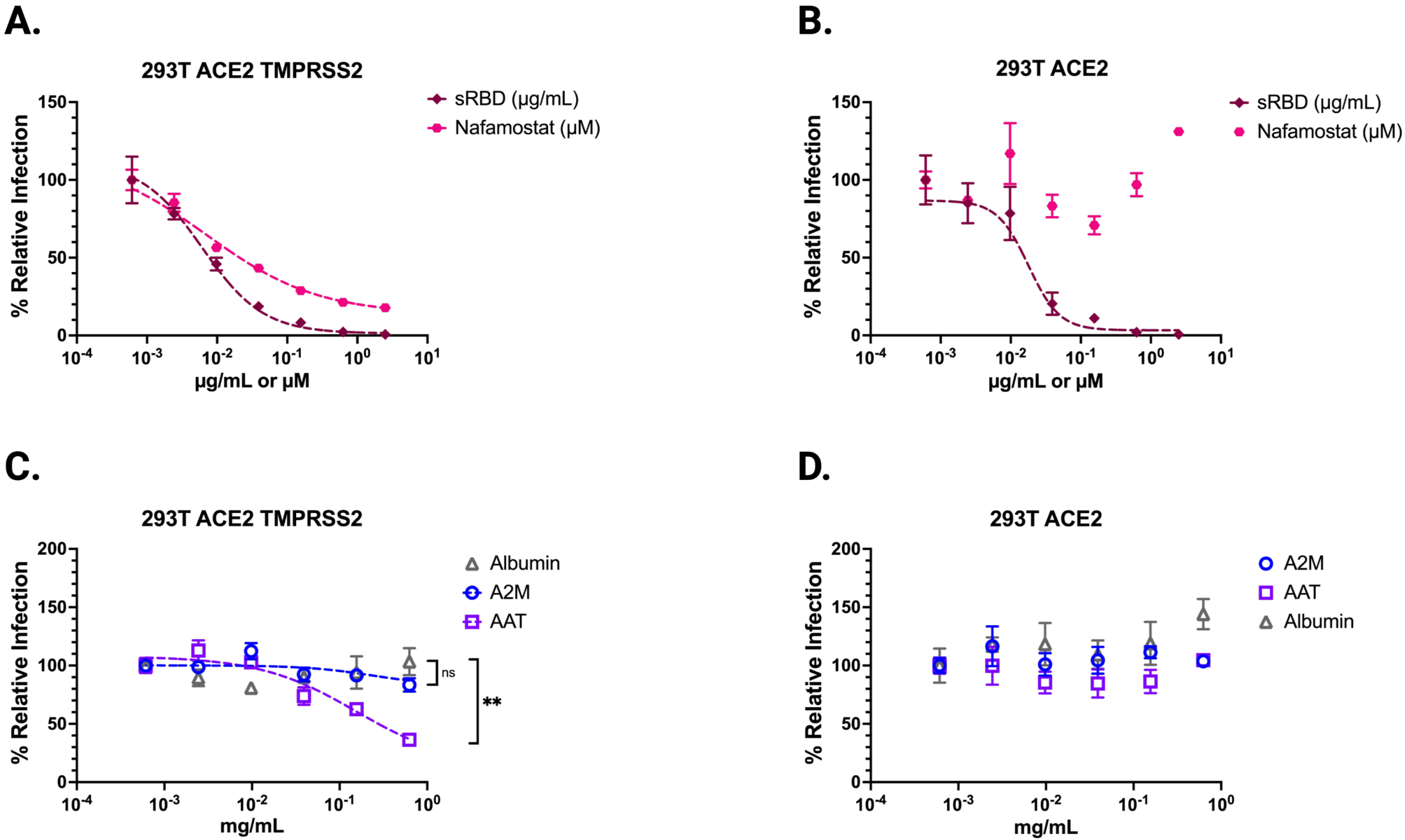
A.
293T ACE2 TMPRSS2
sRBD (µg/mL)
Nafamostat (µM)
% Relative Infection
µg/mL or µM
B.
293T ACE2
sRBD (µg/mL)
Nafamostat (µM)
% Relative Infection
µg/mL or µM
C.
293T ACE2 TMPRSS2
Albumin
A2M
AAT
ns
**
% Relative Infection
mg/mL
D.
293T ACE2
A2M
AAT
Albumin
% Relative Infection
mg/mL

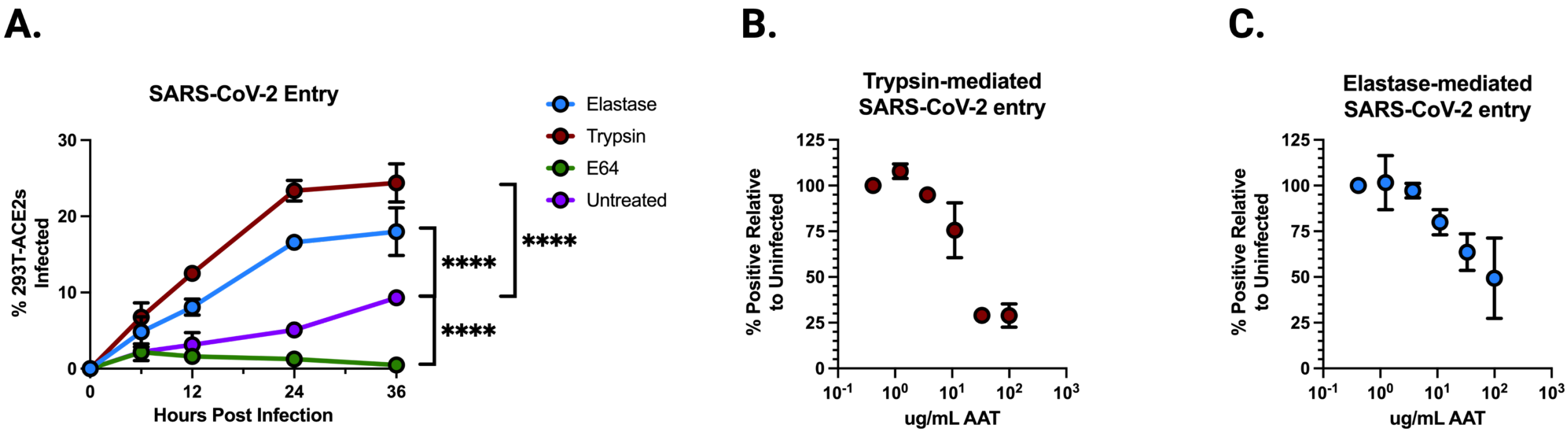
A.
SARS-CoV-2 Entry
% 293T-ACE2s Infected
Hours Post Infection
0
12
24
36
0
10
20
30
****
****
****
Elastase
Trypsin
E64
Untreated
B.
Trypsin-mediated SARS-CoV-2 entry
% Positive Relative to Uninfected
ug/mL AAT
0
25
50
75
100
125
10^{-1}
10^{0}
10^{1}
10^{2}
10^{3}
C.
Elastase-mediated SARS-CoV-2 entry
% Positive Relative to Uninfected
ug/mL AAT
0
25
50
75
100
125
10^{-1}
10^{0}
10^{1}
10^{2}
10^{3}

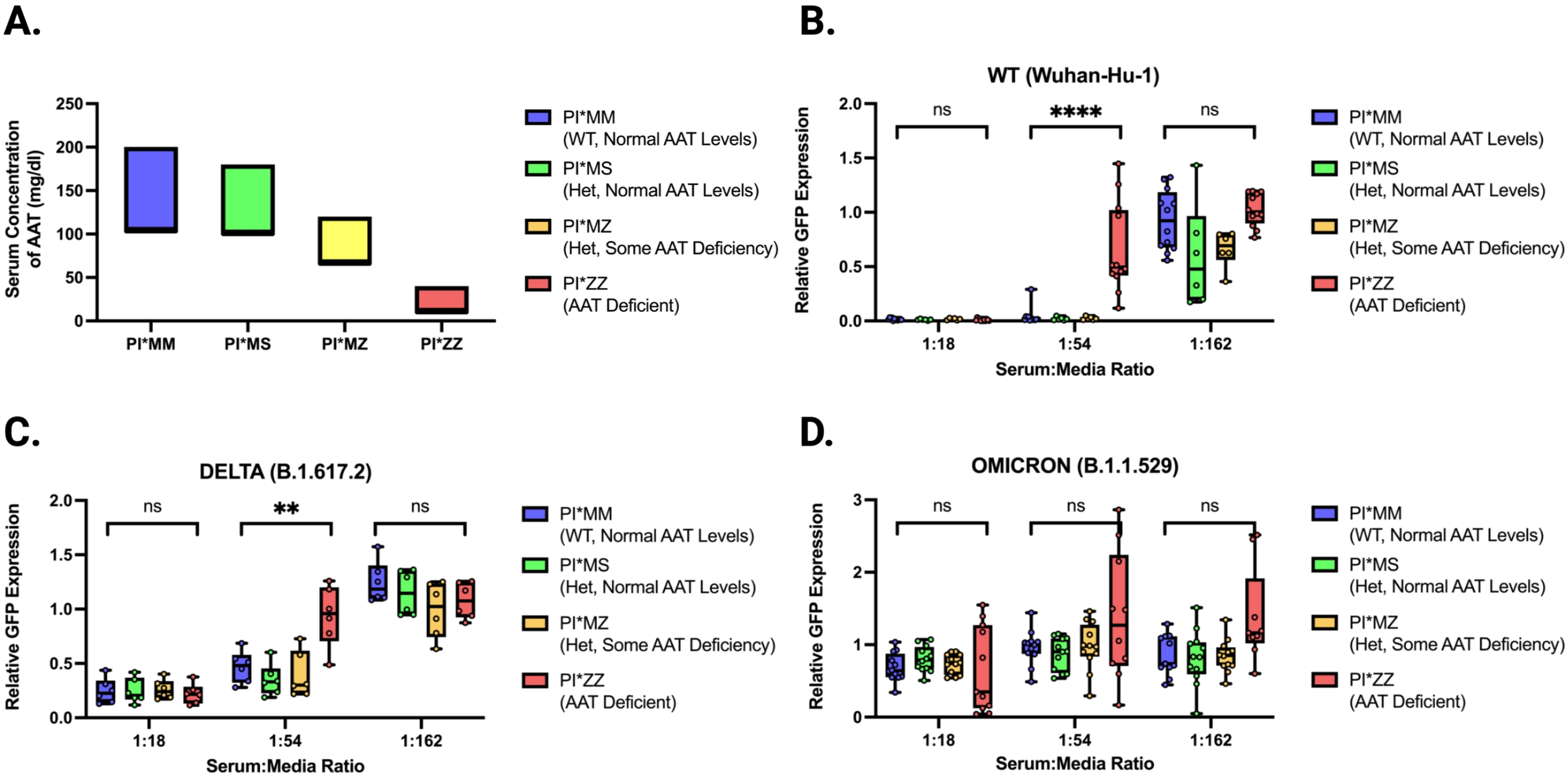
A.
Serum Concentration of AAT (mg/dl)
250
200
150
100
50
0
PI*MM
PI*MS
PI*MZ
PI*ZZ
PI*MM (WT, Normal AAT Levels)
PI*MS (Het, Normal AAT Levels)
PI*MZ (Het, Some AAT Deficiency)
PI*ZZ (AAT Deficient)
B.
WT (Wuhan-Hu-1)
Relative GFP Expression
2.0
1.5
1.0
0.5
0.0
ns
****
ns
1:18
1:54
1:162
Serum:Media Ratio
PI*MM (WT, Normal AAT Levels)
PI*MS (Het, Normal AAT Levels)
PI*MZ (Het, Some AAT Deficiency)
PI*ZZ (AAT Deficient)
C.
DELTA (B.1.617.2)
Relative GFP Expression
2.0
1.5
1.0
0.5
0.0
ns
**
ns
1:18
1:54
1:162
Serum:Media Ratio
PI*MM (WT, Normal AAT Levels)
PI*MS (Het, Normal AAT Levels)
PI*MZ (Het, Some AAT Deficiency)
PI*ZZ (AAT Deficient)
D.
OMICRON (B.1.1.529)
Relative GFP Expression
3
2
1
0
ns
ns
ns
1:18
1:54
1:162
Serum:Media Ratio
PI*MM (WT, Normal AAT Levels)
PI*MS (Het, Normal AAT Levels)
PI*MZ (Het, Some AAT Deficiency)
PI*ZZ (AAT Deficient)